

JAERI-M

9153

THE REACTION OF UNIRRADIATED AND  
IRRADIATED NUCLEAR GRAPHITES  
WITH WATER VAPOR IN HELIUM

October 1980

Hisashi IMAI, Shinzo NOMURA, Takeshi KUROSAWA,  
Kimio FUJII and Yasuichi SASAKI

この報告書は、日本原子力研究所が JAERI-M レポートとして、不定期に刊行している研究報告書です。入手、複製などのお問い合わせは、日本原子力研究所技術情報部（茨城県那珂郡東海村）あて、お申しこしください。

JAERI-M reports, issued irregularly, describe the results of research works carried out in JAERI. Inquiries about the availability of reports and their reproduction should be addressed to Division of Technical Information, Japan Atomic Energy Research Institute, Tokai-mura, Naka-gun, Ibaraki-ken, Japan.

The reaction of unirradiated and irradiated nuclear  
graphites with water vapor in helium

Hisashi IMAI, Shinzo NOMURA, Takeshi KUROSAWA,  
Kimio FUJII and Yasuichi SASAKI

Division of Nuclear Fuel Research,  
Tokai Research Establishment, JAERI

(Received October 2, 1980)

Nuclear graphites more than 10 brands were oxidized with water vapor in helium and then some selected graphites were irradiated with fast neutron in the Japan Materials Testing Reactor to clarify the effect of radiation damage of graphite on their reaction behaviors. The reaction was carried out under a well defined condition in the temperature range  $800 \sim 1000^{\circ}\text{C}$  at concentrations of water vapor 0.38  $\sim$  1.30 volume percent in helium flow of total pressure of 1 atm. The chemical reactivity of graphite irradiated at  $1000 \pm 50^{\circ}\text{C}$  increased linearly with neutron fluence until irradiation of  $3.2 \times 10^{21} \text{ n/cm}^2$ . The activation energy for the reaction was found to decrease with neutron fluence for almost all the graphites, except for a few ones. The order of reaction increased from 0.5 for the unirradiated graphite to 1.0 for the graphite irradiated up to  $6.0 \times 10^{20} \text{ n/cm}^2$ .

Experiment was also performed to study a superposed effect between the influence of radiation damage of graphite and the catalytic action of barium on the reaction rate, as well as the effect of catalyser of barium. It was shown that these effects were not superposed upon each other, although barium had a strong catalytic action on the reaction.

Keywords: Nuclear Graphite, Reaction with Water Vapor, Reaction Rate, Activation Energy, Order of Reaction, Radiation Damage, Catalytic Effect

照射前および照射済み原子炉用黒鉛材料の  
ヘリウム中水蒸気との反応

日本原子力研究所東海研究所燃料工学部  
今井 久・野村 真三・黒沢 武  
藤井貴美夫・佐々木泰一

(1980年10月2日受理)

10種類以上の照射前原子炉用黒鉛材料についてヘリウム中水蒸気による高温の反応試験を行うとともに、その中から数種類の黒鉛材料を選んでJMTRで中性子照射し、照射済み黒鉛材料の反応速度、反応速度の温度依存性、および反応次数等におよぼす放射線損傷の影響を調べた。実験は直径11mm、長さ50mmの試験片を使用し、全圧1気圧、650ml/minのヘリウム気流中で実施した。反応温度は800~1000°C、水蒸気濃度範囲は0.38~1.30%である。

1000±50°Cで中性子照射された黒鉛材料の1000°Cにおける反応速度は照射量の増加とともに直線的に増加したが、 $3.2 \times 10^{21} \text{ n/cm}^2$ の照射量でも照射前の値の2倍を超えることはなかった。反応の活性化エネルギーは大部分の黒鉛材料では照射によって減少したが、含有不純物量の多い一部の黒鉛材料では逆に増加したものがあつた。反応の次数は照射前黒鉛材料は0.5であつたが、1000°Cで $6.0 \times 10^{20} \text{ n/cm}^2$ まで照射された材料では1.0で、照射により増加した。

また、反応におよぼすバリウムの触媒作用について調べるため、バリウムを添加した黒鉛材料についても実験を行った。バリウムはきわめて強い正触媒で反応速度を加速するが、高温の黒鉛表面では不安定で蒸発しやすく、その触媒作用は時間の経過とともに減少することが明らかになった。さらに放射線損傷の影響とバリウムの触媒効果が相乗して作用し、互の効果を強め合うことがないことを確認した。

## CONTENTS

1. Introduction .....	1
2. Experimental .....	2
2.1 Materials .....	2
2.1.1 Graphite .....	2
2.1.2 Gas .....	2
2.2 Apparatus .....	3
2.3 Procedure .....	3
3. Basic consideration .....	4
4. Results and discussion .....	5
4.1 Rate of reaction .....	5
4.1.1 Unirradiated and irradiated graphites .....	5
4.1.2 Catalysis of barium .....	8
4.2 Temperature dependence of reaction rate .....	10
4.3 Order of reaction .....	12
4.4 Product gas .....	14
5. Summary .....	16
Acknowledgements .....	17
References .....	18

## 目 次

1. まえがき	1
2. 実 験	2
2.1 試 料	2
2.1.1 黒鉛材料	2
2.1.2 反応ガス	2
2.2 使用装置	3
2.3 実験操作	3
3. 予備的考察	4
4. 結果と考察	5
4.1 反応速度	5
4.1.1 照射及び照射済み黒鉛材料	5
4.1.2 バリウムの触媒作用	8
4.2 反応速度の温度依存性	10
4.3 反応次数	12
4.4 生成ガス	14
5. 総 括	16
謝 辞	17
参考文献	18

## 1. INTRODUCTION

In the design of the Very High Temperature Gas Cooled Reactor planned at Japan Atomic Energy Research Institute, the outlet temperature of the coolant helium is expected to be 1000°C under operating condition. This means that the surface temperature of graphite components will be around 1200°C and the condition is very severe for the corrosion of the core graphite materials. The weight loss of graphite components due to corrosion will result in decrease of their mechanical strength and also their thermal conductivity, which could lead to a safety related consequence. In the reactor core environment, there might be an irradiation enhancement of the corrosion rate by the creation of new chemical active sites in the graphite and also by the formation of active species of gaseous impurities in helium. The chemical reactivity of graphite itself during irradiation, however, might not be expected to increase so much, because the created active sites would be annealed out at high temperatures in the reactor. The yield of active species resulted from the radiolysis of impurity gas (G value) will be increased in helium through the so-called Penning effect which is the secondary transfer of energy from excited helium to impurity gas.<sup>(1)</sup> It is therefore important to obtain a better understanding on the corrosion behavior of graphite under the reactor operating condition. The present studies were made by an out-of-pile experimental apparatus to obtain the reaction data of graphites with water vapor in helium gas, and the effects of radiation damage in graphite materials caused by fast neutron irradiation on the corrosion reaction of graphite with humidified helium are described.

## 2. EXPERIMENTAL

### 2.1 Materials

#### 2.1.1 Graphite

Nuclear graphites used in the experiment are listed along with some of their characteristics in Table 1. These graphites were classified into two groups of the gilso-carbon and of the petroleum-coke base graphites according to their starting raw material. Each group was further subdivided into extruded graphites and pressed (or molded) ones according to the manufacturing process employed. Cylindrical specimens 50.0 mm length and 11.0 mm diameter were used; their average weight and the geometrical surface area were 8.5 g and 20.0 cm<sup>2</sup>, respectively (Fig.1). From a large block of graphite, 15 specimens were cut out so as to eliminate the specimen-to-specimen variation in graphite samples as much as possible. The longer side of each specimen was cut parallel to extrusion or perpendicular to pressing. The apparent density, electrical resistivity and Young's modulus were measured for all 15 specimens of each graphite brand, and the specimens having the values within the standard deviation among them were selected and used for this study. The surface of each specimen was washed with carbon tetrachloride of reagent grade and dried for 160 hours in a clean atmosphere at 120°C. The specimens were irradiated in the Japan Materials Testing Reactor up to  $3.2 \times 10^{21}$  n/cm<sup>2</sup> ( $E > 0.18$  MeV) over the temperature range between 800 ~ 1200°C.

#### 2.1.2 Gas

Helium of six nine grade in purity was used without purification. A certain amount of water vapor was fed from distilled water to the



helium. The contents of oxygen and the other impurity gas in the humidified helium were kept less than 0.1 and 1 vpm, respectively.

## 2.2 Apparatus

The apparatus used in the experiment is schematically shown in Fig.2. In order to avoid radioactive contamination in the laboratory, only the reaction part of the apparatus was set in a low pressure box (Fig.3). The most part of the apparatus consisted of Pyrex glass tubes, except for the high temperature reaction part, which was made of a silica glass tube. The helium gas containing water vapor was preheated by passing through a silica glass wool packed in the section just ahead of the specimen and then flowed to react over the heated graphite. The helium-water vapor mixture was prepared by bubbling of the helium through the distilled water kept at a controlled temperature. During the reaction, the concentration of water vapor in helium was continually monitored by a moisture meter. At the outlet, the gas was released into the atmosphere through a mercury sealing device. The reaction temperature was automatically controlled by a regulator of an accuracy of  $\pm 1^\circ\text{C}$ . The reaction products were analyzed by a gaschromatograph equipped with two kinds of detectors of helium ionization and of flame ionization. The flame ionization detector was provided with nickel catalyser column for analysis of carbon mono and dioxide, in which both the gases were reduced to methane.

## 2.3 Procedure

The cylindrical specimen mounted on a four points holder was set in the reaction tube and heat-treated at  $1000^\circ\text{C}$  in a vacuum of  $10^{-3}$  pascal.

for several hours prior to the reaction, in order to eliminate surface complexes and adsorbates on its surface. Pre-oxidation treatment for the graphites were not carried out. Before starting the reaction, the dry helium was introduced into the reaction tube heated up to a pre-determined reaction temperature, and then the reaction was initiated by mixing of water vapor into the dry helium flow of total pressure of 1 atmosphere. A fraction of gas passed through the reaction tube was led into the gaschromatograph for analysis at regular intervals. The reaction was carried out at a gas flow rate, above which no further increase in the reaction rate was found. The gas flow rate was 650 ml/min which corresponded to a linear flow rate of 5.7 cm/sec over the specimen surface.

### 3. BASIC CONSIDERATION

It is known that in high temperature reaction of graphite with water vapor, there are two kinds of the primary reactions (1), (2) and of the main secondary ones (3), (4) as follows:



Values of the equilibrium constants for the primary and secondary reactions are presented in Table 2.<sup>(2)</sup> In the gasification of graphite by corrosive gas, the following empirical informations are known for the progress of reaction in connection with the Gibbs' free energy,  $\Delta F$ ,<sup>(3)</sup>

where  $-\Delta F$  is expressed by the well known formula,  $RT \ln K$ .

- i)  $\Delta F < 0$  ; The reaction easily proceeds.
- ii)  $0 < \Delta F < 10$  Kcal/mole ; The gasification can proceed, but not easily.
- iii)  $10$  Kcal/mole  $< \Delta F$  ; The reaction can proceed only under a favorable condition.

The corrosion of graphite with water vapor is expected to proceed easily at temperatures above  $700$  °C.

#### 4. RESULTS AND DISCUSSION

##### 4.1 Rate of reaction

##### 4.1.1 Unirradiated and irradiated graphites

Hydrogen, as well as carbon monoxide, was found to be the primary product in the reaction of graphite with water vapor at high temperatures. Carbon dioxide and hydrocarbons were also found in the product gas, but they were a small amount compared with the primary product gases at high temperatures. The reaction rate was calculated from the yields of gaseous carbon compounds formed in the reaction and the flow rate of the gas. Only the specimens cut parallel to extrusion or perpendicular to pressing was employed in the experiment, because it was found in the preliminary study that the grain orientation in specimen gave very little effect on the rate of reaction. The reaction rate at  $1000$  °C rapidly increased in the initial stage of reaction and then gradually turned a mild rising (Fig.4a). The increase of reaction rate with the reaction time can be ascribed to development of the surface area caused by the reaction, because the reaction rate of 7477PT graphite was found

to increase in proportion to increasing of the surface area as shown in Table 3. For the unirradiated graphites the reaction rates were found to be in a range  $0.4 \sim 3.0 \text{ mg/cm}^2 \cdot \text{hr}$  at  $1000 \text{ }^\circ\text{C}$  under 0.65 volume percent water vapor in the helium for 10 hours (Table I). Only the 7477 graphite showed a pronounced high rate, although the rates of the other graphites were less than  $1.0 \text{ mg/cm}^2 \cdot \text{hr}$ .

The reaction rate at temperatures lower than  $950 \text{ }^\circ\text{C}$  went through a maximum value at a very initial stage and showed a mild increasing with the elapse of reaction time again (Fig.4b). It is known from the result in Fig.4b that there might be two kinds of carbon atoms in reactivity, the active and the less active. The higher rate in the initial stage can be regarded to be due to the reaction of the active carbon atom. The active carbon atom was consumed in the initial stage of reaction as seen in Fig.4b, but the higher rate was reproduced in the second run on the same specimen which has been heat-treated in vacuum at  $1000 \text{ }^\circ\text{C}$  after the reaction. It is therefore considered that the active carbon is not anything like powder which was formed through shaping process of the specimen but the active atom on the surface of graphite specimen. Desorption treatment for the reacted graphite at high temperatures may enable to reform from the less active atom to the active carbon one because of removal of the edge carbon atoms accompanied with desorption of chemisorbed foreign atoms<sup>(4,5,6)</sup>. However, the difference in reactivity between the active and the less active did not appear in the reaction at  $1000 \text{ }^\circ\text{C}$  because of the increase of reaction rate of the less active carbon atom. The reaction rate of unirradiated 7477PT graphite under 0.65 volume percent water vapor showed  $30 \text{ } \mu\text{g/cm}^2 \cdot \text{hr}$  at  $900 \text{ }^\circ\text{C}$  and  $1 \text{ } \mu\text{g/cm}^2 \cdot \text{hr}$  at  $800 \text{ }^\circ\text{C}$  in each steady state of the reaction.

The reaction rate of 7477PT graphite irradiated at  $1000 \pm 50 \text{ }^\circ\text{C}$  is

shown in Fig.5 as function of carbon gasified during the reaction at 0.65 volume percent water vapor concentration at 1000 °C. The rates of reaction for the irradiated graphites were higher than those of the un-irradiated ones in the same kind of graphite, except for the SMI-24 graphite. The results for SMI-24 graphite are shown in Fig.6. It was impossible to determine the irradiation effect on the reaction rate of SMI-24 graphite because of some scatters of the rates of the unirradiated ones. It can be also seen in Fig.5 that the chemical reactivity increases with neutron fluence for the graphite irradiated at  $1000 \pm 50$  °C. Fig.7 shows a relation between neutron fluence and the reaction rate of 7477PT graphite, in which the reaction rates are plotted for each burn-off of 1, 5 and 10 mg/cm<sup>2</sup>. The reactivity of 7477PT graphite irradiated at  $1000 \pm 50$  °C increased linearly with neutron fluence until irradiation of  $3.2 \times 10^{21}$  n/cm<sup>2</sup>. The reaction rate of 7477PT graphite can be expressed with neutron fluence as follows:

$$R(\text{mg}/\text{cm}^2 \cdot \text{hr}) = 8.6 \times 10^{-23} F + 0.21 \quad \text{for } 1 \text{ mg}/\text{cm}^2 \text{ burn-off (5)}$$

$$R(\text{mg}/\text{cm}^2 \cdot \text{hr}) = 9.5 \times 10^{-23} F + 0.32 \quad \text{for } 5 \text{ mg}/\text{cm}^2 \text{ burn-off (6)}$$

$$R(\text{mg}/\text{cm}^2 \cdot \text{hr}) = 10.0 \times 10^{-23} F + 0.42 \quad \text{for } 10 \text{ mg}/\text{cm}^2 \text{ burn-off (7)}$$

where R is the reaction rate and F is the fluence of neutron (n/cm<sup>2</sup>) above 0.18 MeV. The fluence dependence of the reaction rate (that means the slope of line in Fig.7) slightly increased with progress of burn-off. In Fig.8, the reaction rates of various graphites irradiated up to  $3.2 \times 10^{21}$  n/cm<sup>2</sup> at 950 °C were shown as a function of burn-off (mg/cm<sup>2</sup>). The reaction behavior of the irradiated graphite (the shape of line in Fig.8) was similar to that of the unirradiated one of the same kind of graphite. Fig.9 shows the same relation as Fig.7 for three kinds of

graphites, in which only the reaction rate at  $1 \text{ mg/cm}^2$  burn-off was plotted. It is observed that the effect of irradiation was the largest for 7477PT graphite, but the rate did not go up to over twice that of the unirradiated one, even at a neutron fluence of  $3.2 \times 10^{21} \text{ n/cm}^2$ . It was also found that irradiation gave less effect on the reaction rates of IE1-24 and H327 when they were compared with the 7477PT graphite. The 7477PT seems to be one of the graphites which easily makes the new chemical active sites in it during neutron irradiation.

The reaction rate of 7477PT graphite irradiated at  $1200 \text{ }^\circ\text{C}$  is given along with one irradiated at  $1040 \text{ }^\circ\text{C}$  in Fig.10, although their neutron fluence is not equal for each irradiation temperature. The reaction rate of the graphite irradiated at  $1200 \text{ }^\circ\text{C}$  seems to have a lower value of 70 ~ 80 percent to the graphite irradiated at  $1040 \text{ }^\circ\text{C}$ , if they would be compared at a same neutron fluence. It is considered that the lower rate of reaction for the graphite irradiated at the higher temperature is due to annealing of the radiation damage in the graphite. Some experimental equations which showed a relation between the reaction rate and burn-off were formulated to fit for the behavior of reaction at  $1000 \text{ }^\circ\text{C}$  (Table 4). The reaction rate at any burn-off will be able to be calculated by these equations. It must be recognized that the coefficients in the equations differed from graphite to graphite and also changed with neutron fluence.

#### 4.1.2 Catalysis of barium

Barium is well known as one of the typical fission product having a strong catalytic action on the reaction of graphite with water vapor.<sup>(7)</sup> The fission product can participate in the reaction of the surface by the migration through the graphite structure materials such as the fuel

sleeve. From a point of view described above, study on barium catalysis was also carried out using the pure graphite, 7477PT to avoid the catalytic effect of the other impurity contained in graphite. Contamination of the specimen was conducted by a vacuum impregnation method using barium hydroxide solution and the impregnated specimen was dried for 24 hours in a clean air at 120 °C. And then the contaminated specimen was heated for 4 hours in a vacuum to intercalate barium into the graphite crystallite. Although most of the barium was vaporized through the heating process at 1000 °C, it was confirmed by X-ray diffraction analysis that a part of the barium formed an intercalation in the graphite.

Fig.11 shows the reaction behavior of the unirradiated 7477PT graphite contaminated with barium, as well as that of the non-contaminated graphite. The concentration of barium in the examined specimen was  $13 \mu\text{g}/\text{cm}^2$  in geometrical surface area and the reaction temperature was 1000 °C. The barium in unirradiated graphite made the chemical reactivity increase by a factor of 20 in the initial stage of the reaction at 1000 °C but the rate decreased down with the reaction time in contrast with the behavior of the non-contaminated graphite. This decrease of the rate means reduction of the barium concentration on the surface of graphite with progress of the reaction. In gasification of graphite, it is generally known that metal impurity contained in graphite is accumulated as ash on the surface of graphite during the reaction and its reaction rate is accelerated due to the catalytic action of ash with the elapse of time. Thus, the result obtained here indicates that barium ash is not able to exist in a stable form on surface of graphite under high temperatures. It was found that there were a number of pits on the surface of reacted barium-graphite and the reaction locally proceeded.

The reaction at 1000 °C was also carried out on the irradiated graphite contaminated with barium, the graphite of which has been irradiated up to  $2.0 \times 10^{21}$  n/cm<sup>2</sup> with fast neutron at 950 °C (Fig.12). The catalytic effect appeared only in the initial stage of reaction and the reaction rate soon decreased down to the level of that of the irradiated graphite without barium. It is considered from this result that there is no superposed effect between the enhancement by radiation damage and the acceleration by catalysis.

There will be very little barium on the surface of graphite structure materials in the reactor during the operation, comparing with the concentration of barium used in this experiment. It may therefore be concluded that barium in the fission products does not make any trouble on the graphite corrosion in the reactor environment.

#### 4.2 Temperature dependence of reaction rate

The experiment was carried out in the temperature range 800 ~ 900 °C at the concentration of water vapor of 0.65 volume percent in helium. The apparent energy of activation for the reaction was found to be in a range 45 ~ 90 Kcal/mole for the unirradiated graphite. In general, the graphite containing much more impurities in quantity had the lower energy of activation than the purified one. The apparent activation energy for the 7477PT graphite irradiated at  $1000 \pm 50$  °C was given as a function of neutron fluence in Fig.13. The activation energy of 7477PT graphite gradually decreased with fluence and the value seemed to result in about 70 percent that for the unirradiated one when irradiation went on. Temperature dependence of the reaction rate was lowered by irradiation for almost all the graphites, but those for a few graphites such as the 7477 and the IM2 increased in contrast to the majority.



The following mechanisms are considered for the change of the apparent energy of activation.

- (1) Change of the heat of adsorption of the irradiated graphite for the reactant gas; the following relation is held,  $E_a = E - Q$ , where  $E_a$  and  $E$  are the apparent and true energies of activation, and  $Q$  is the heat of adsorption for the gas.<sup>(8)</sup>
- (2) Change in the catalysis activity of impurity contained in the graphite which can affect carbon gasification. It is known that the catalysis activity changes by irradiation.<sup>(9)</sup>
- (3) In the gas-graphite reaction, the activation energy is known to change with the pre-exponential factor which corresponds to the concentration of active site.<sup>(10)</sup> A relation,  $mE - \ln A = \text{constant}$  is held, where  $m$  is a proportional constant and  $A$  is the pre-exponential factor in the Arrhenius equation,  $\text{rate} = A \exp(-E/RT)$ .
- (4) There is a temperature difference between reaction spot and matrix substance in the heterogeneous reaction such as graphite-gas. The heat of reaction would lead the reaction spot to various temperatures corresponding to the rate of reaction and the temperature difference can give various activation energies on the same reaction.<sup>(11)</sup>

It is very difficult to show clearly the mechanism which caused the change of apparent energy of activation, because it is considered to have changed by complex combination among the four phenomena above-mentioned. However, the decrease of apparent energy of activation may be mainly ascribed to increase of the heat of adsorption for water vapor which resulted from disordering introduced in the graphite crystallite by neutron irradiation. On the other hand, the increase of energy with

fluence, which is observed for the reactions of 7477 and IM2 graphites, may be correlated with impurity in the graphite. Both the graphites have contained much more impurity, especially vanadium and nickel, in quantity than the other graphites. Ash in the majority graphites are 300 ppm or less, while both the 7477 and the IM2 graphites contain about 1000 ppm ash. The apparent energy of activation for various graphites were shown as a part of the rate equation in Table 5. Contamination with barium lowered the apparent energy of activation for the reaction. The unirradiated 7477PT graphite with  $3 \mu\text{g}/\text{cm}^2$  barium showed an activation energy of 32 Kcal/mole, but this value would change with barium content.<sup>(10)</sup>

#### 4.3 Order of reaction

There is a general agreement that experimental data on the rate of reaction of graphite by water vapor fit an equation of Langmuir-Hinshelwood type as follows:

$$\text{Rate} = \frac{k_1 C_{\text{H}_2\text{O}}}{1 + k_2 C_{\text{H}_2} + k_3 C_{\text{H}_2\text{O}}} \quad (4)$$

where  $C_{\text{H}_2\text{O}}$  and  $C_{\text{H}_2}$  are the concentrations of water vapor and hydrogen, and the constants  $k_1$ ,  $k_2$  and  $k_3$  are functions of one or more rate constants. Here,  $C_{\text{H}_2}$  is zero in this study since there is no hydrogen in the reactant gas. Thus a simple equation is obtained from the reciprocal of the equation (4).

$$\frac{1}{\text{Rate}} = K + \frac{1}{k_1 C_{\text{H}_2\text{O}}} \quad (5)$$

where K shows  $k_3/k_1$ .

The order of reaction was measured at concentrations of water vapor between 0.38 and 1.30 volume percent at 1000 °C which was considered to be the upper temperature of chemical controlled regime. The irradiated and unirradiated IE1-24 graphites were used for this purpose, in which the former have been irradiated up to  $6.0 \times 10^{20}$  n/cm<sup>2</sup> with fast neutron at 1000 °C. In accordance with the equation (5), the relationship of 1/Rate (1/mg/min) with  $1/C_{\text{H}_2\text{O}}$  (1/vol.%) was plotted by using the experimental data as shown in Fig.14, which gave straight lines in the range of experimental concentration. The following rate equations were obtained from analysis of the lines in Fig.14.

$$\text{Rate} = \frac{1.17 \times 10^{-4} C_{\text{H}_2\text{O}}}{1 + 1.43 \times 10^{-4} C_{\text{H}_2\text{O}}} \quad \text{for the unirradiated graphite} \quad (6)$$

$$\text{Rate} = 1.34 \times 10^{-4} C_{\text{H}_2\text{O}} \quad \text{for the irradiated graphite} \quad (7)$$

The influences of water vapor concentration on the reaction rate were more understandably shown in Fig.15, in which the reaction rates were plotted as a function of water vapor concentration on log-log scale. These plots give straight lines and the following relation can be obtained.

$$\text{Rate} = k(C_{\text{H}_2\text{O}})^n \quad (8)$$

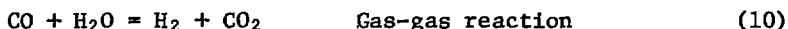
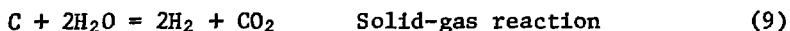
where k is the constant and n shows the order of reaction. The order of reaction at 1000 °C increased from 0.5 to 1.0 by irradiation of  $6.0 \times 10^{20}$  n/cm<sup>2</sup> at 1000 °C. The order of 1.0 for the irradiated graphite can be also known from the equation (7). There would be two

factors which lead to increase of the order of reaction<sup>(12)</sup>: the one is increase of release rate of the surface complex formed during the reaction and the other is increase of the active surface area of the irradiated graphite. It is, however, difficult to consider that the release rate of surface complex increase in the reaction of irradiated graphite. Disordering of crystallite lattice which was introduced by irradiation would rather serve to slow down the release rate of surface complex on the graphite. The increase of the order of reaction may be ascribed to increase of the active surface area of graphite. The dependence of the order upon the reaction temperature was not studied, but it is known that the order is insensitive with change of the reaction temperature.<sup>(13,14)</sup>

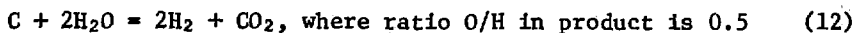
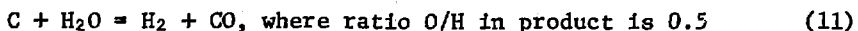
#### 4.4 Product gas

In the reaction at high temperatures, a small amount of carbon dioxide was found in the product gases which were mainly composed of hydrogen and carbon monoxide. The fraction of carbon dioxide in the product gas, however, changed for each graphite and also by irradiation of graphite in the reaction at the same experimental condition. The graphite containing much more impurity generally showed the formation of a significant amount of carbon dioxide than the purified one. There was trace amount of carbon dioxide in the reaction of unirradiated 7477PT graphite at 1000 °C, but the unirradiated 7477, which contained much more impurity than 7477PT, formed carbon dioxide of 15 volume percent in the total product gas. Carbon dioxide also increased in the reaction of the irradiated 7477PT graphite as seen in Fig.16, the graphite in which was irradiated up to  $3.2 \times 10^{21}$  n/cm<sup>2</sup> at 950 °C.

The ratio  $\text{CO}_2/\text{CO}$  for the irradiated 7477PT graphite was 0.18 at 1000 °C and increased up to about 0.75 at 815 °C with decreasing of the reaction temperature, while that for the unirradiated one showed only 0.04 of  $\text{CO}_2/\text{CO}$  even at 815 °C. There are two ways for the formation of carbon dioxide in the reaction of graphite with water vapor as follows:



where the carbon monoxide in the gas-gas reaction (10) is formed in the primary reaction (1). If carbon dioxide were produced in the gas-gas reaction, it should be significantly found even in the product gas for the unirradiated 7477PT graphite. It is, therefore, considered that carbon dioxide was formed in the solid-gas reaction as the equation (9). Fig.17 shows both atomic ratios of O/H in the product gases for the unirradiated and irradiated 7477PT graphites as a function of the time in the reaction at 1000 °C. The ratio O/H for the irradiated graphite was much less than 0.5 in the initial stage of the reaction and gradually approached to 0.5 line with the elapse of reaction time. On the other hand, the ratio O/H for the unirradiated graphite showed 0.5 except in the very initial stage of the reaction. As seen in the following chemical equations (11) and (12), the ratio O/H in the product should always be 0.5.



The less ratio than 0.5, therefore, indicates that some of the oxygen form relatively stable surface complexes on the graphite in the primary

attack with water vapor as the follows,



where C(O) represents the carbon-oxygen surface complex. It is difficult to consider the formation of C(O<sub>2</sub>) surface complex in the primary attack, because water molecule consists of an oxygen atom. Thus, it is considered that carbon dioxide is formed in the secondary attack with water vapor as the follows,



It was also found that there was a close relation between the reaction rate and the ratio CO<sub>2</sub>/CO as shown in Fig.18, in which the reaction rates at 1000 °C were plotted as a function of the ratio CO<sub>2</sub>/CO in the steady state. The ratio CO<sub>2</sub>/CO for the 7477PT graphite, as well as the reaction rate, increased with neutron fluence. And also the reaction rates of the various graphites irradiated at the same condition are found to be associated with the ratio of CO<sub>2</sub>/CO. These results may indicate that the oxygen in the equation (13) is chemisorbed on the lattice site which has been damaged by irradiation of fast neutron. The 7477PT graphite, which showed the highest ratio of CO<sub>2</sub>/CO among the graphites irradiated up to  $3.2 \times 10^{21}$  n/cm<sup>2</sup>, must be one of the graphites damaged easily, and this consideration is consistent with the results shown in Fig.9.

## 5. SUMMARY

1. The reaction rate of unirradiated graphites were found to be 0.4~0.9 mg/cm<sup>2</sup>·hr for 10 hours at 0.65 volume percent water vapor in helium at 1000 °C, except for 3.0 mg/cm<sup>2</sup>·hr of the 7477 graphite.

2. In the reaction at 1000 °C, the rates of graphites irradiated at  $1000 \pm 50$  °C increased linearly with neutron fluence, but the rates did not go up over twice those of the unirradiated graphites at a neutron fluence of  $3.2 \times 10^{21}$  n/cm<sup>2</sup>. The higher irradiation temperature seems to give a less effect on the reaction rate, when the rate is measured on the graphite irradiated up to the same neutron fluence.
3. The dependence of the reaction rate on temperature decreased with increase of the neutron fluence for almost all the graphites, except for a few graphites. The apparent energy of activation for the reaction of 7477PT graphite was regarded to converge to 70 percent of that for the unirradiated graphite when the neutron irradiation was allowed to continue.
4. The order of reaction was measured in the range of water vapor between 0.38 and 1.30 volume percent at 1000 °C. The order increased from 0.5 for the unirradiated graphite to 1.0 after the irradiation of  $6.0 \times 10^{20}$  n/cm<sup>2</sup> at 1000 °C.
5. The ratio of carbon dioxide to monoxide in the product gas increased by the irradiation and there was a close relation between the reaction rate and the ratio of CO<sub>2</sub>/CO.
6. Barium in the graphite greatly accelerated the reaction rate at 1000 °C. In the reaction of irradiated graphite contaminated with barium, however, a superposed effect on the reaction rate was not able to be found between the enhancement by radiation damage and the acceleration by barium.

#### ACKNOWLEDGEMENTS

The authors would like to thank Head of Nuclear Fuel Research Division, Dr. Junichi Shimokawa for his encouragements.

## REFERENCES

1. M.R. Everett, D.V. Kinsey and E. Römberg, Chemistry and Physics of Carbon, Vol.3, 362, Marcel-Decker, New York (1968)
2. N.V. Lavrov, V.V. Korobov and V.I. Filippova, The Thermodynamics of Gasification and Gas-Synthesis reactions, 93, Pergamon Press, Oxford, London, New York, Paris (1963)
3. 米田幸二, 牧島象二, 工業ガス, 岩波講座, 現代化学, 岩波書店
4. L. Bonnetain, J. Chim. Phys., Vol.56, 266 (1959)
5. *ibid.*, 486 (1959)
6. L. Bonnetain, X. Duval and M. Letort, Proceedings 4th Conf. Carbon, 107, Buffalo, New York (1960)
7. M.B. Peroomian, A.W. Barsell and J.C. Saeger, GA-A12493, January (1974)
8. 田村幹雄, 物理化学, 下巻, 至文堂 (昭和38年)
9. H.E. Frausworth and R.F. Woodcock, Advances in Catalysis, Vol.9, 123 (1957)
10. P.L. Walker, Jr., M. Shelef and R.A. Anderson, Chemistry and physics of Carbon, Vol.4, 308 (1968)
11. J.C. Lewis, 2nd Conf. Industrial Carbon and Graphite, 258, Society of Chemical Industry, London (1966)
12. P.L. Walker, Jr., Frank Rusinko, Jr., and L.G. Austin, Advances in Catalysis, Vol.11, 133 (1959)
13. J.P. Blakely and L.G. Overholser, Carbon, Vol.2, 385 (1965)
14. *ibid.*, Vol.3, 269 (1965)



Table 1. Characteristics of nuclear graphites

Brand	Raw Material	Compaction Method	Ash (ppm)	Apparent Density (g/cm <sup>3</sup> )	Butanol Density (g/cm <sup>3</sup> )	c <sub>o</sub> (002) (Å)	a <sub>o</sub> (110) (Å)	L <sub>c</sub> (002) (Å)	BAF <sup>a)</sup>	Reaction <sup>b)</sup> Rate (mg/cm <sup>2</sup> hr)
SEG-RM-H	Needle Coke	Extrusion	—	1.70	2.222	6.723	2.463	780	1.68	0.8
SMG	Needle Coke	Extrusion	20	1.75	2.209	6.726	2.462	470	1.10	1.6
G163AS	Needle Coke	Extrusion	20	1.76	2.169	6.723	2.462	740	1.17	0.8
IE1-24	Gilsonite Coke	Extrusion	200	1.82	2.180	6.733	2.462	340	1.08	0.4
IM2	Gilsonite Coke	Molding	1000	1.78	2.211	6.742	2.461	330	1.01	0.7
IM2-24	Gilsonite Coke	Molding	200	1.76	2.167	6.752	2.461	330	—	0.5
SE2-24	Needle Coke	Extrusion	170	1.72	2.206	6.730	2.463	530	1.15	0.8
H327	Needle Coke	Extrusion	300	1.77	2.227	6.721	2.462	640	1.49	0.4
7477	Fine Needle Coke	Molding	1000	1.75	2.149	6.734	2.461	450	1.04	3.0
7477PT	Fine Needle Coke	Molding	5	1.74	2.155	6.733	2.461	450	1.00	0.6
SM1-24	Needle Coke	Molding	200	1.78	2.219	6.735	2.461	420	1.05	0.9
IG-11	Fine Needle Coke	Molding	40	1.79	2.177	6.741	2.461	370	1.00	0.6

a) Bacon Anisotropic Factor.

b) Under 0.65 % water vapor in helium, at 1000°C, for 10 hours

Table 2 Equilibrium constants for graphite-water vapor and associated reactions

T (K)	$K_p$			
	$C + H_2O =$ $= CO + H_2$	$C + 2H_2O =$ $= CO_2 + 2H_2$	$CO + H_2O =$ $= CO_2 + H_2$	$C + 2H_2 =$ $= CH_4$
298.16	$9.525 \times 10^{-17}$	$9.891 \times 10^{-12}$	$1.038 \times 10^5$	$7.918 \times 10^8$
400	$7.339 \times 10^{-11}$	$1.136 \times 10^{-7}$	$1.548 \times 10^3$	$3.146 \times 10^5$
500	$2.217 \times 10^{-7}$	$3.043 \times 10^{-5}$	$1.372 \times 10^2$	$2.676 \times 10^3$
600	$4.813 \times 10^{-5}$	$1.361 \times 10^{-3}$	28.274	$1.001 \times 10^2$
700	$2.288 \times 10^{-3}$	$2.154 \times 10^{-2}$	9.4126	8.929
800	$4.183 \times 10^{-2}$	0.1765	4.2191	1.403
900	0.403	0.9251	2.2972	0.3230
1000	2.4689	3.5345	1.4316	$9.799 \times 10^{-2}$
1100	10.9078	10.7363	0.9843	$3.650 \times 10^{-2}$
1200	37.6051	27.3540	0.7274	$1.476 \times 10^{-2}$
1300	$1.069 \times 10^2$	60.5268	0.5657	$7.868 \times 10^{-3}$
1400	$2.616 \times 10^2$	$1.201 \times 10^2$	0.4591	$4.290 \times 10^{-3}$

Table 3 Changes of reaction rate and surface area with progress of reaction at 1000°C for 7477PT graphite

Burn-off (mg/cm <sup>2</sup> )	Reaction rate (mg/cm <sup>2</sup> . hr)	Specific surface area (m <sup>2</sup> /g)	Increase of reaction rate ( $\frac{\text{Reacted}}{\text{Initial}}$ )	Increase of specific surface area ( $\frac{\text{Reacted}}{\text{Initial}}$ )
0	0.06	0.24	—	—
0.4	0.20	0.81	3.33	3.38
2.0	0.36	1.41	6.00	5.88
4.6	0.43	1.76	7.17	7.33

Table 4 Relations between reaction rate and burn-off in reaction at 0.65% H<sub>2</sub>O, at 1000°C.

Brand	Irradiation (n/cm <sup>2</sup> )	Relation
7477PT	—————	$R = -0.00578B^2 + 0.06080B + 0.30492 - 0.02879/B$
SM1-24	—————	$R = -0.00341B^2 + 0.09434B + 0.52432 - 0.07461/B$
IM2-24	—————	$R = -0.00009B^2 + 0.01627B + 0.84226 - 2.46973/B$
7477PT	$3.2 \times 10^{21}$ at 950°C	$R = -0.00180B^2 + 0.05820B + 0.72780 - 0.01366/B$
SM1-24	$1.2 \times 10^{21}$ at 950°C	$R = -0.00078B^2 + 0.01932B + 0.63041 - 0.17558/B$
H327	$3.2 \times 10^{21}$ at 950°C	$R = -0.00683B^2 + 0.08834B + 0.38340 - 0.01359/B$

R = Reaction rate in mg/cm<sup>2</sup>.hrB = Burn-off in mg/cm<sup>2</sup>

Table 5 Rate equations for various graphites

Brand	Irradiation (n/cm <sup>2</sup> )	Rate equation (mg/cm <sup>2</sup> .hr)
7477PT	—————	$2.7 \times 10^{14} \exp(-87,000/RT)$
7477	—————	$5.5 \times 10^7 \exp(-46,000/RT)$
SM1-24	—————	$1.3 \times 10^{12} \exp(-73,000/RT)$
IM2-24	—————	$3.0 \times 10^{14} \exp(-92,000/RT)$
IM2	—————	$4.7 \times 10^{10} \exp(-62,000/RT)$
H327	—————	$4.6 \times 10^{14} \exp(-88,000/RT)$
7477PT	$3.2 \times 10^{21}$ at 950°C	$1.3 \times 10^{11} \exp(-63,000/RT)$
7477	$6 \times 10^{20}$ at 1000°C	$2.1 \times 10^{12} \exp(-74,000/RT)$
SM1-24	$1.2 \times 10^{21}$ at 950°C	$2.0 \times 10^{12} \exp(-70,000/RT)$
IM2	$6 \times 10^{20}$ at 1000°C	$2.1 \times 10^{14} \exp(-81,000/RT)$
H327	$6 \times 10^{20}$ at 1000°C	$4.7 \times 10^{11} \exp(-81,000/RT)$

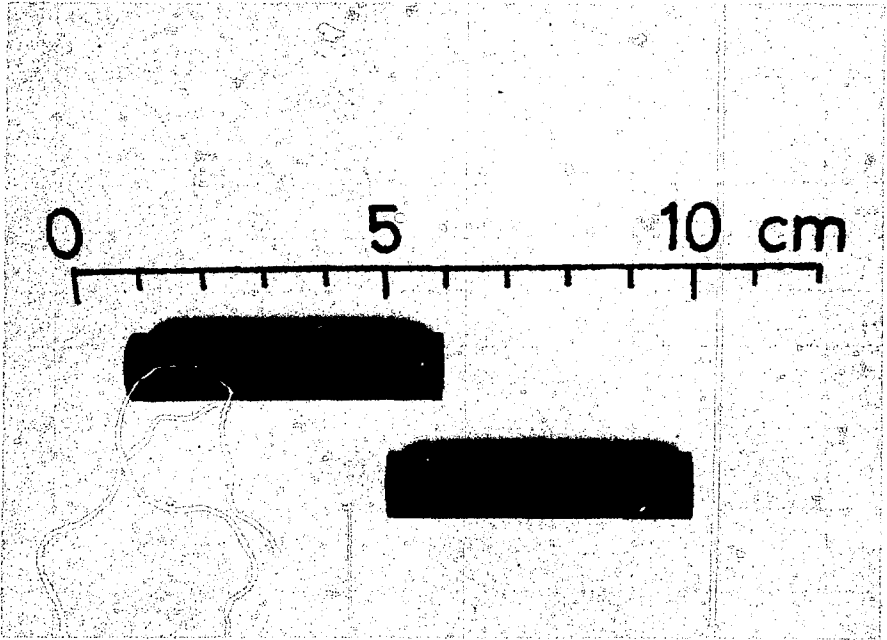


Fig. 1 Specimens used in high temperature reaction

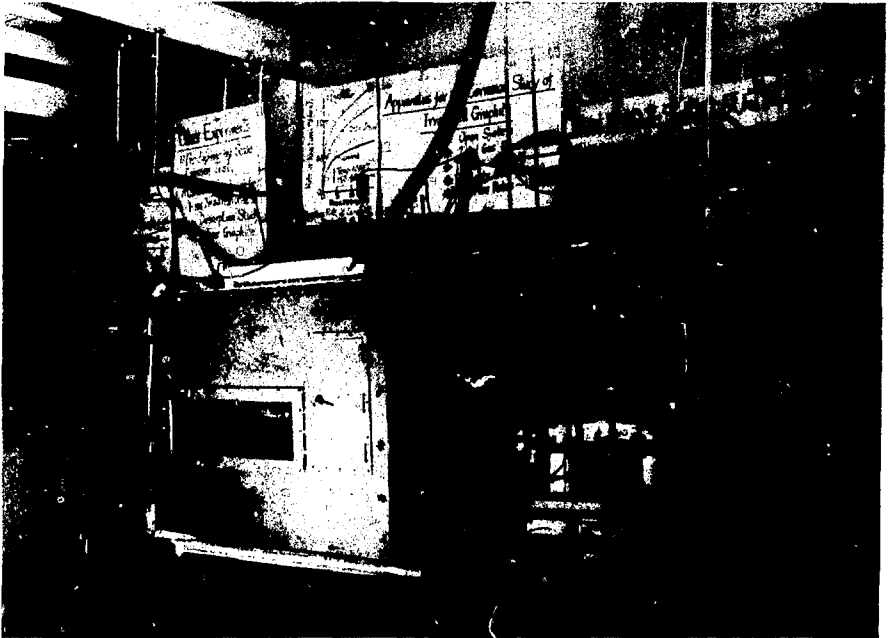


Fig. 3 Whole view of reaction apparatus and furnace in box

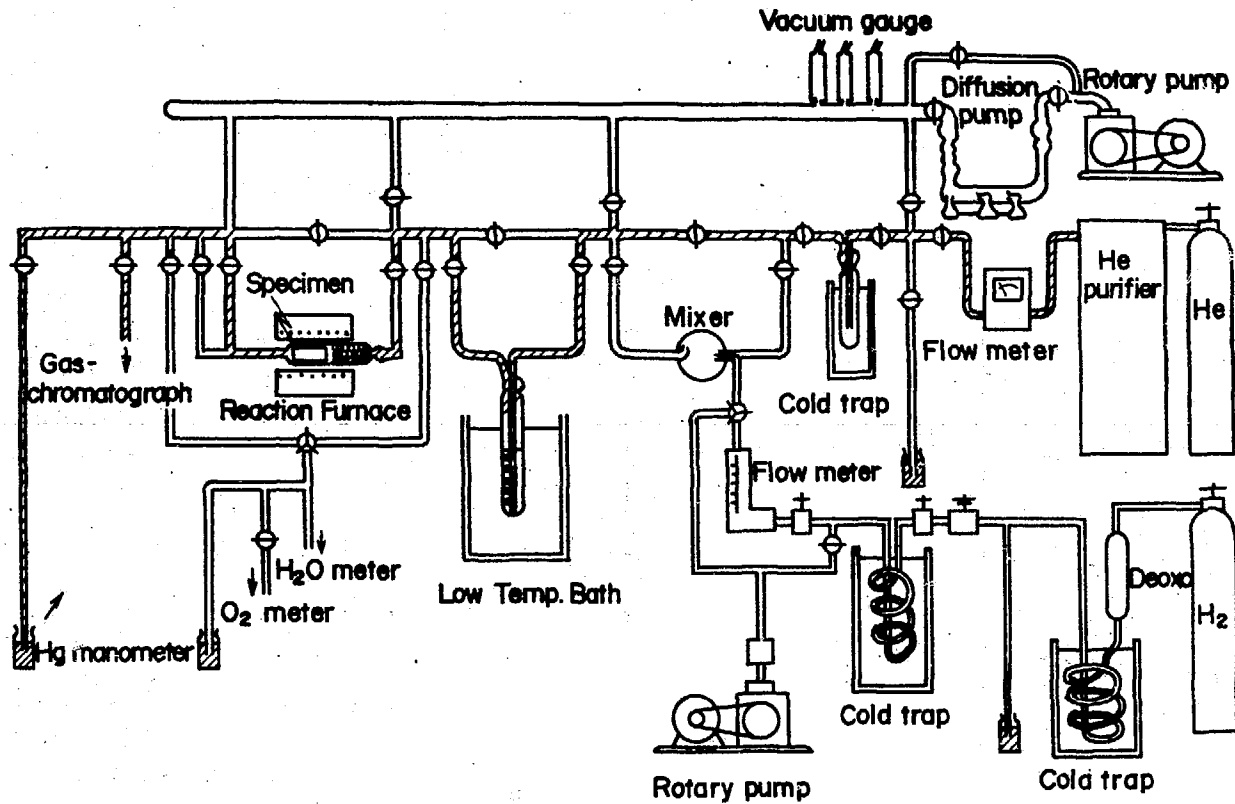


Fig. 2 Apparatus for reaction of graphite with water vapor in helium

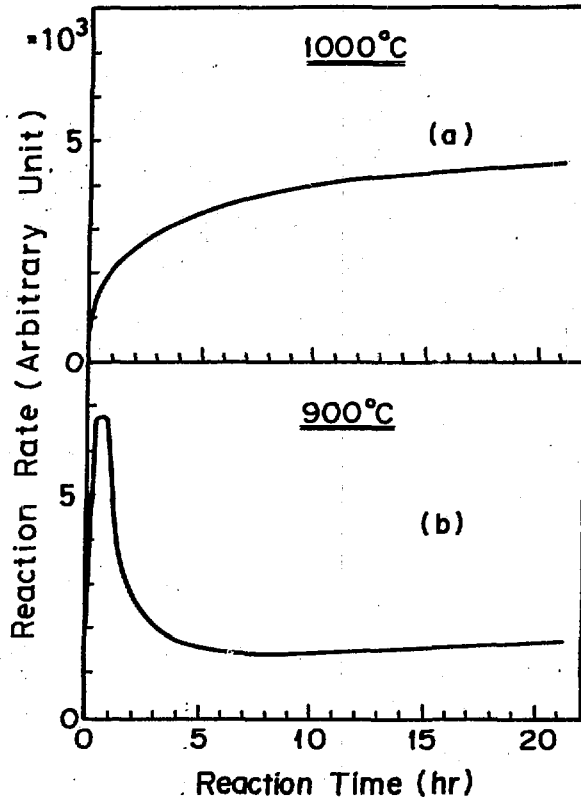


Fig. 4 Typical behaviors of reaction of graphite with water vapor at 900 and 1000 °C

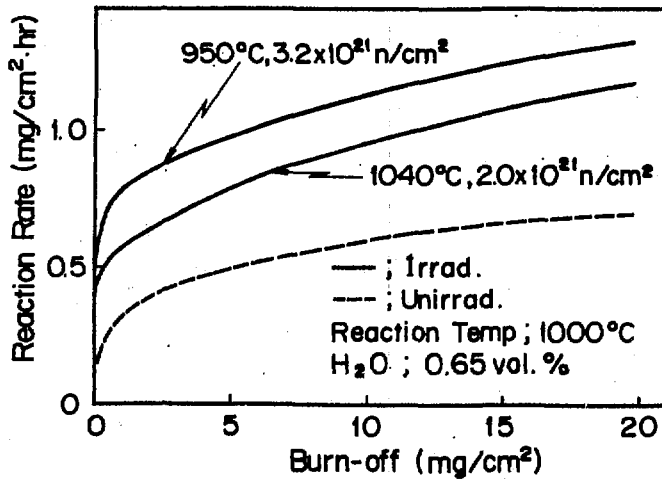


Fig. 5 Reaction rate of 7477PT graphite at 1000 °C and 0.65% of water vapor in helium

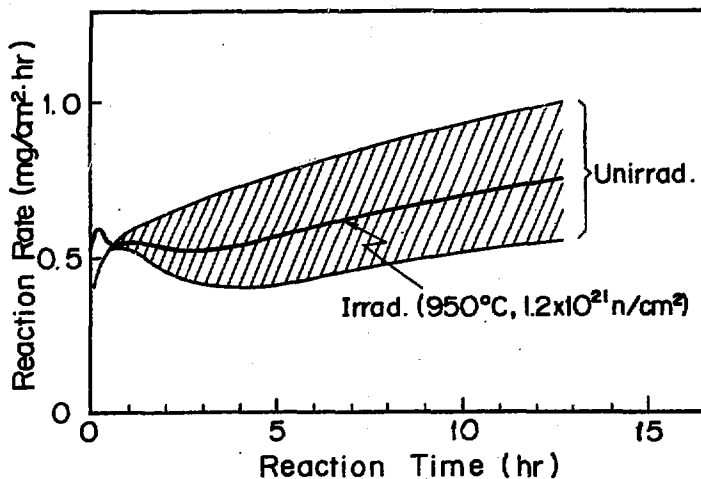


Fig. 6 Reaction rate of SMI-24 graphite at 1000 °C and 0.65% of water vapor in helium

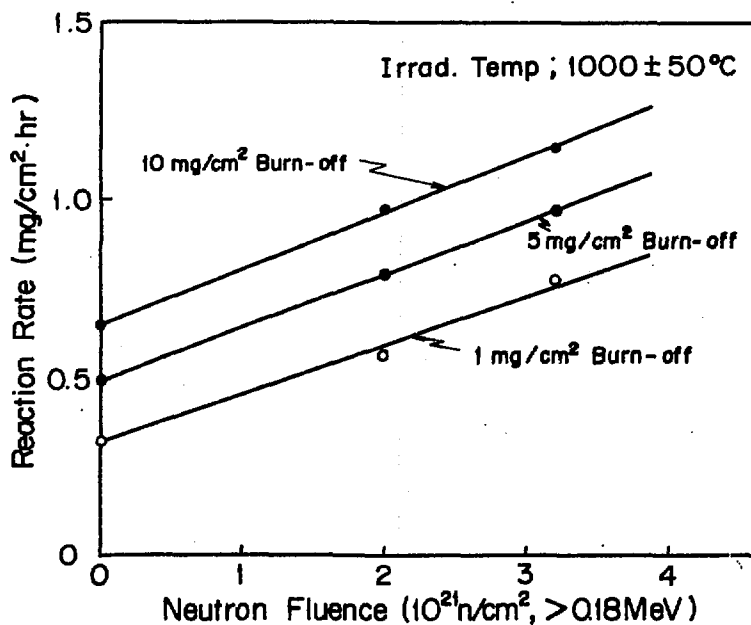


Fig.7 Effect of neutron fluence on reaction rate of 7477 PT graphite at 1000°C and 0.65% of water vapor in helium.

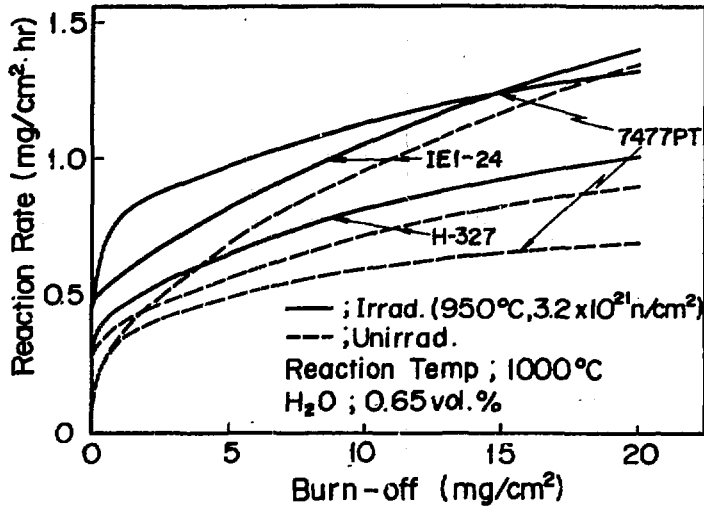


Fig. 8 Reaction rates of irradiated graphites at 1000 °C and 0.65% of water vapor in helium

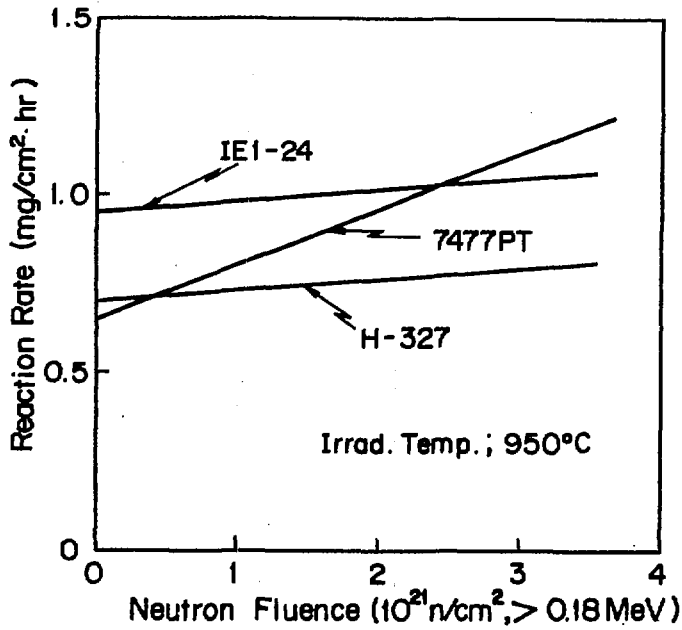


Fig.9 Effect of neutron fluence on reaction rates of various graphites at 1000 °C and 0.65% of water vapor in helium.



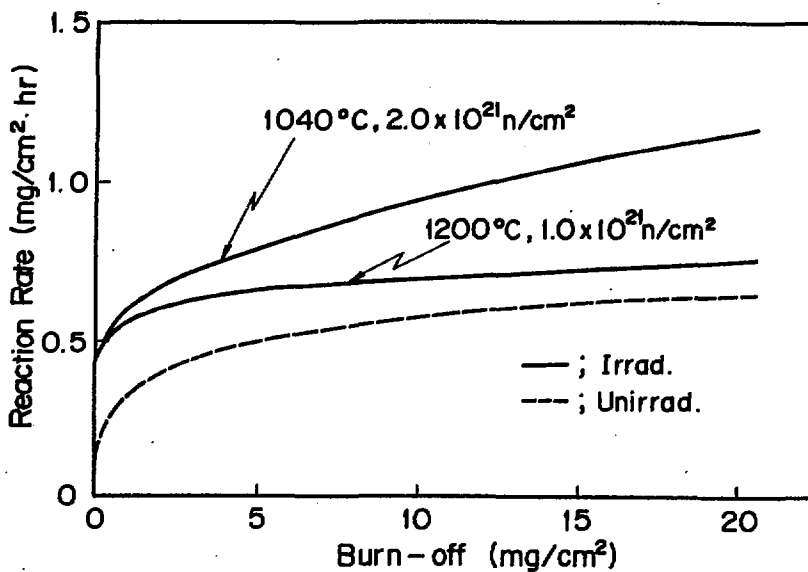


Fig. 10 Reaction rate of irradiated 7477PT graphites at 1000°C and 0.65% of water vapor in helium.

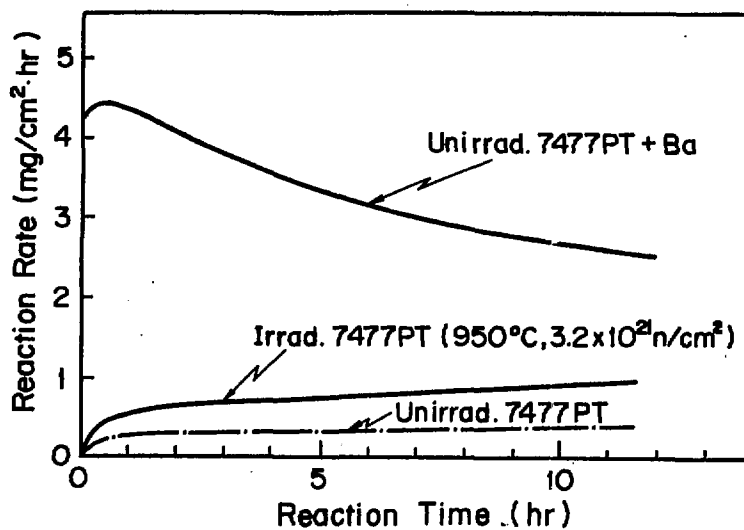


Fig. 11 Reaction rate of barium contaminated 7477PT graphite at 1000°C and 0.65% of water vapor in helium.

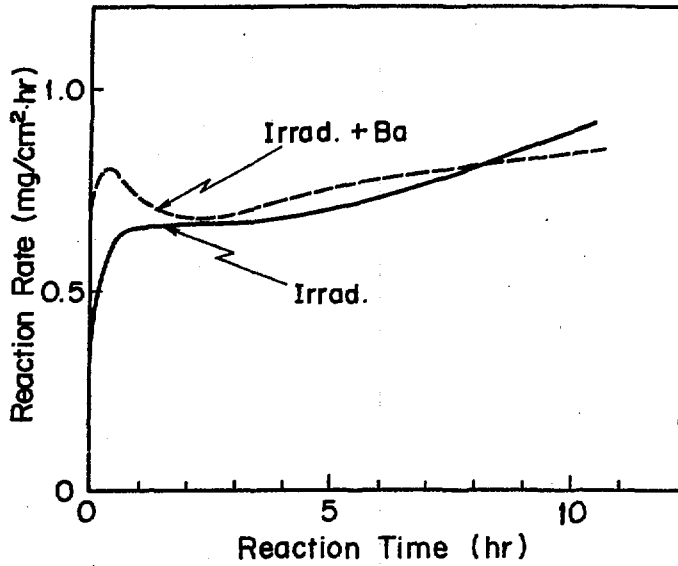


Fig.12 Reaction rate of irradiated graphite contaminated with barium at 1000°C and 0.65% of water vapor in helium.

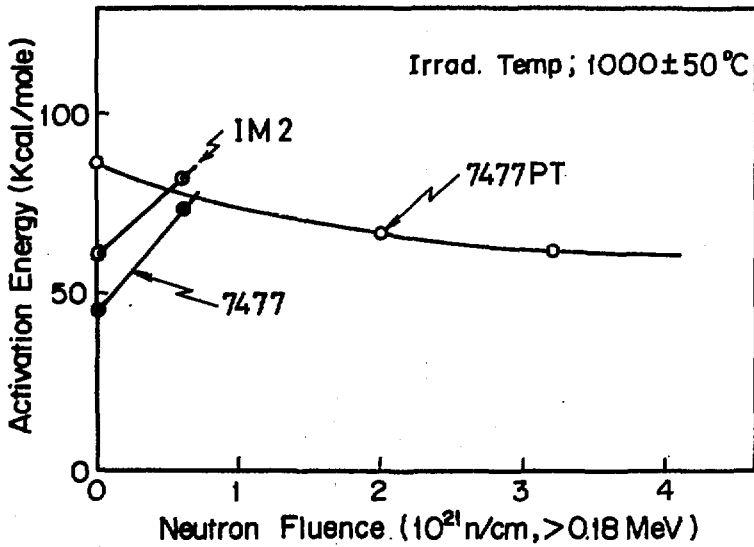


Fig.13 Change of activation energy for reaction as a function of neutron fluence.

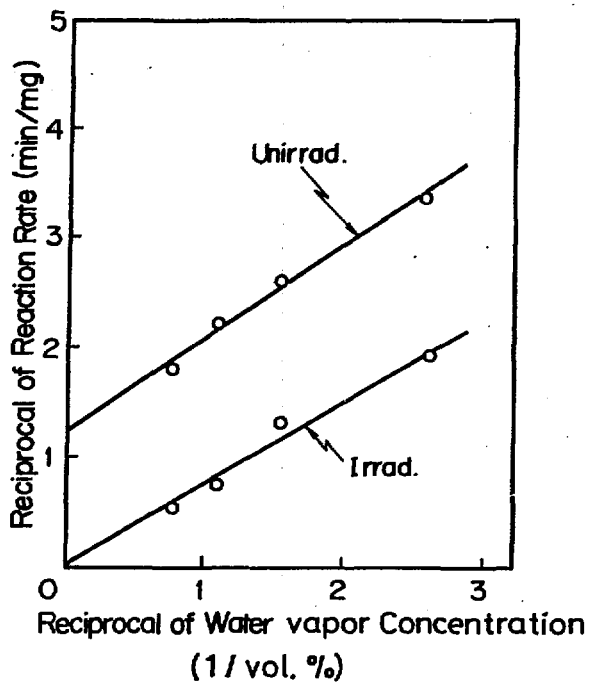


Fig.14 Relation between reciprocal of reaction rate and reciprocal of water vapor concentration .

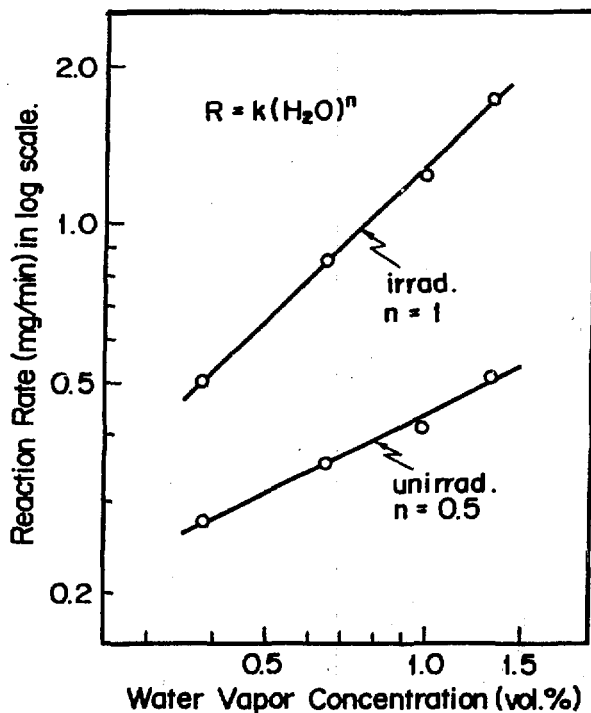


Fig.15 Relation between reaction rate and water vapor concentration .

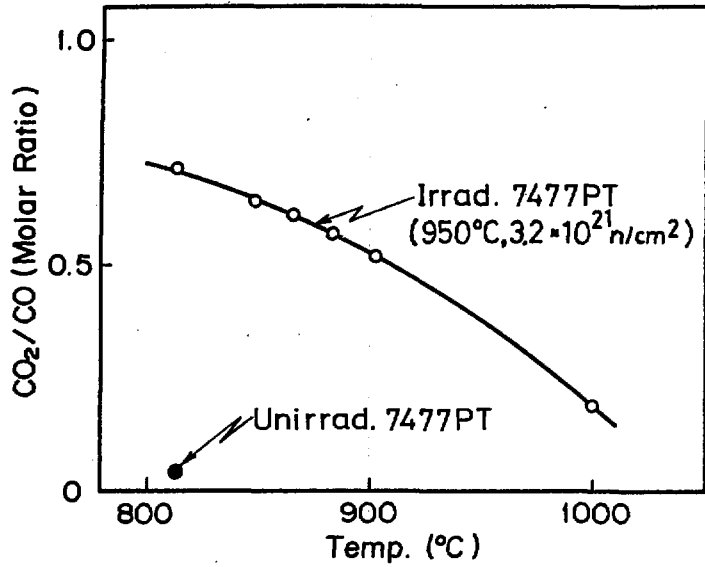


Fig.16 Change of  $\text{CO}_2/\text{CO}$  in product gas as a function of reaction temperature.

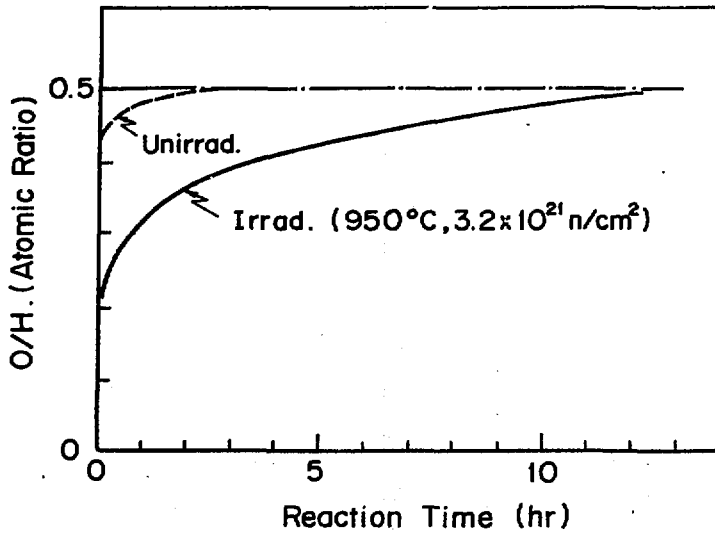


Fig.17 Change of  $\text{O}/\text{H}$  in product gas as a function of reaction time.

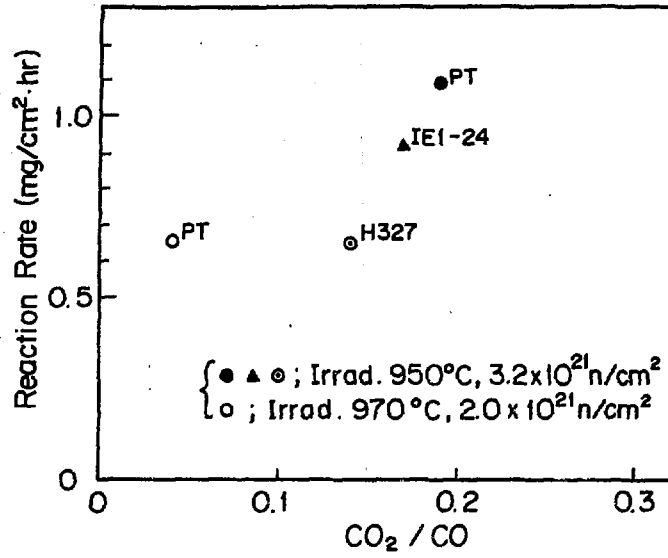


Fig.18 Relation between reaction rate and CO<sub>2</sub>/CO ratio in product gas at 1000°C and 0.65 % of water vapor in helium.